16th World Congress in Computational Mechanics (WCCM)
21-26 July 2024, Vancouver, Canada
A. Korobenko, M. Laforet, S. Prudhomme, R. Vaziri (Eds)

COMPLETE VARIABLE KINEMATIC CUF-BASED MULTILAYERED SHELL ELEMENTS.

E. CARRERA[1], D. SCANO[2]

[1]DIMEAS, Politecnico di Torino
C.so Duca Degli Abruzzi 24, Turin, Italy
erasmo.carrera@polito.it

[2] DIMEAS, Politecnico di Torino
C.so Duca Degli Abruzzi 24, Turin, Italy
daniele.scano@polito.it

Key words: Finite element method, shell models, composite structures, locking-free elements, Carrera Unified Formulation.

Abstract. The paper presents a methodology for formulating multi-layered composite shell theories with arbitrary kinematic fields. Each displacement variable is examined through an independent expansion function, allowing integration of equivalent single layer and layer-wise approaches within the Carrera Unified Formulation. Finite element method discretizes the structure in the reference plane of the plate using Lagrange-based elements. Governing equations are derived using the principle of virtual displacements. The study considers multilayered structures with different radius-to-thickness ratios and compares results with analytical solutions from the literature. Findings suggest the most appropriate model selection depends strongly on specific problem parameters.

1 INTRODUCTION

Shell structures are vital in engineering due to their efficient load-bearing capabilities. However, advancements in structural materials like composites have led to more complex designs, requiring rigorous analyzes and resulting in increased computational expenses.

The complexity of analyzing these structures primarily arises from anisotropic nature, leading to intricate mechanical phenomena. These problems include challenges such as ensuring continuity between layers for shear components and meeting zig-zag distribution requirements for displacements, commonly known as C^0_z requirements [1]. The combination of out-of-plane and in-plane strain components increases the intricacy.

In the last decades, various shell models have been proposed. The first and less computationally intensive two-dimensional (2D) model is known as Thin Shell Theory (TST), detailed in [2]. It is assumed that that the section of the shell remains orthogonal to the reference surface during deformation. The First Shear Deformation Theory (FSDT) was developed to account for transverse shear deformation. It originated from the works of Reissner [3] and Mindlin [4]. Thus, the classical theories cannot accurately study such structures.

Scholars proposed several refined theories for composite structures, employing two primary modelling techniques: the Equivalent-Single Layer (ESL) and the Layer Wise (LW)

approaches. In the ESL approach, mathematical assumptions regarding the displacement field remain consistent across all layers. See for instance Kant et al. [5] and Reddy [6]. Consequently, the resulting model encompasses variables for the entire composite structure. Conversely, the LW approach involves distinct variables described in each layer, while ensuring mechanical characteristics' continuity at the interlaminar level. Notable works include those by Reddy [7], and Noor and Burton [8].

The primary objective of this study is to approach shell analysis from a new perspective, wherein each displacement field can be approximated using an appropriate structural theory. For instance, employing advanced LW theories for in-plane displacements and ESL models for transverse displacements. The Carrera Unified Formulation (CUF) [9,10,11] serves as the tool enabling the implementation of each theory in a simple and hierarchical manner within a Finite Element (FE) framework. The novel CUF uses nine scalar Fundamental Nuclei, whose formulation does not change with the chosen kinematic theory.

To counteract the shear and membrane locking of the FE methods, the Mixed Interpolation of Tensorial Components is implemented in the formulation [12]. Cinefra and Carrera [13] first included this integration scheme in the CUF framework.

This paper is structured as follows: (a) Section 2 presents several classical and refined shell theories from the open literature. Also, Taylor-based, and Lagrange-like expansions are illustrated. In particular, the concept of mixed ESL/LW approach is explained. (b) Section 3 illustrates the principles of the Unified formulation approximation and the union with the finite element method. (c) In Section 4, the governing equations are derived, and it shows how to assemble the stiffness matrix and the load vector. (e) In Section 5, results for cylindrical shells are shown. (f) Finally, the main conclusions are reported in Section 6.

2 REVIEWS OF THE SHELL THEORIES

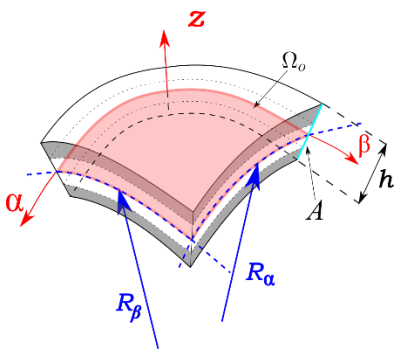

Figure 1: Reference system for a generic multi-layered structure.

Consider the multi-layered shell illustrated in Fig. 1, the two-dimensional (2D) model employs a curvilinear reference system. The curvatures are denoted as R_α and R_β. Specifically, section A is oriented along the thickness direction z. Thus, the mid-plane Ω_0 is placed in the $\alpha - \beta$ plane of the structure. The three-dimensional (3D) displacement field is as follows:

$$\mathbf{u}^k(\alpha,\beta,z) = \{u_\alpha^k(\alpha,\beta,z), \quad u_\beta^k(\alpha,\beta,z), \quad u_z^k(\alpha,\beta,z)\}^T \tag{1}$$

Each component of the displacement variable, namely u_α^k, u_β^k, and u_z^k can be examined with different expansions. Consequently, this section explicitly outlines several theories, spanning

from classical to more advanced higher-order models.

2.1 Classical and literature shell theories

One of the simplest models is the Thin Shell Theory (TST), see [2]. The three displacement components are described in the followings:

$$\begin{aligned} u_\alpha(\alpha,\beta,z) &= u_{\alpha1}(\alpha,\beta) - \frac{\partial u_{z1}(\alpha,\beta)}{\partial\alpha} z \\ u_\beta(\alpha,\beta,z) &= u_{\beta1}(\alpha,\beta) - \frac{\partial u_{z1}(\alpha,\beta)}{\partial\beta} z \\ u_z(\alpha,\beta,z) &= u_{z1}(\alpha,\beta) \end{aligned} \tag{2}$$

Next, the First-order Shear Deformation Theory (FSDT) introduces slight additional complexity. Further details can be found in references [3, 4]. The displacement field is expressed as follows:

$$\begin{aligned} u_\alpha(\alpha,\beta,z) &= u_{\alpha1}(\alpha,\beta) + \varphi_\beta(\alpha,\beta) z \\ u_\beta(\alpha,\beta,z) &= u_{\beta1}(\alpha,\beta) + \varphi_\alpha(\alpha,\beta)\, z \\ u_z(\alpha,\beta,z) &= u_{z1}(\alpha,\beta) \end{aligned} \tag{3}$$

Specifically, $u_{\alpha1}$, $u_{\beta1}$, and u_{z1} represent the displacements of the shell's reference mid-surface in the α, β, and z directions, respectively. The terms φ_β and φ_α denote the rotations about β and α axes. Conversely, the expressions $-\frac{\partial u_{z1}(\alpha,\beta)}{\partial\alpha}$ and $-\frac{\partial u_{z1}(\alpha,\beta)}{\partial\beta}$ describe the rotations, assuming shear deformation is neglected.

The literature works have dealt also with the Higher-Order Theories (HOTs). For instance, Lo et al. [14] proposed the following well-known model:

$$\begin{aligned} u_\alpha(\alpha,\beta,z) &= u_{\alpha0}(\alpha,\beta) + z\psi_\alpha(\alpha,\beta) + z^2\zeta_\alpha(\alpha,\beta) + z^3\phi_\alpha(\alpha,\beta) \\ u_\beta(\alpha,\beta,z) &= u_{\beta0}(\alpha,\beta) + z\psi_\beta(\alpha,\beta) + z^2\zeta_\beta(\alpha,\beta) + z^3\phi_\beta(\alpha,\beta) \\ u_z(\alpha,\beta,z) &= u_{z0}(\alpha,\beta) + z\psi_z(\alpha,\beta) + z^2\zeta_z(\alpha,\beta) \end{aligned} \tag{4}$$

2.2 Taylor-based Higher-order theories

Moreover, Taylor polynomials in the form z^b, where b is a positive integer, may be used to develop Higher-Order Theories (HOTs) for analyzing shell behavior. Within the CUF framework, Carrera [15] pioneered the exploration of such polynomials for shells. This advancement enables the incorporation of higher-order effects in the analysis. These theories and the classical ones are ESL models.

In the literature concerning CUF applied to shell formulations, it is customary to assume a consistent expansion across all three displacement variables. This approach leads to what are referred to as uniform theories. For instance, a fourth-order theory might be outlined as follows:

$$\begin{aligned} u_\alpha(\alpha,\beta,z) &= u_{\alpha1}(\alpha,\beta) + zu_{\alpha2}(\alpha,\beta) + z^2u_{\alpha3}(\alpha,\beta) + z^3u_{\alpha4}(\alpha,\beta) + z^4u_{\alpha5}(\alpha,\beta) \\ u_\beta(\alpha,\beta,z) &= u_{\beta1}(\alpha,\beta) + zu_{\beta2}(\alpha,\beta) + z^2u_{\beta3}(\alpha,\beta) + z^3u_{\beta4}(\alpha,\beta) + z^4u_{\beta5}(\alpha,\beta) \\ u_z(\alpha,\beta,z) &= u_{z1}(\alpha,\beta) + zu_{z2}(\alpha,\beta) + z^2u_{z3}(\alpha,\beta) + z^3u_{z4}(\alpha,\beta) + z^4u_{z5}(\alpha,\beta) \end{aligned} \tag{5}$$

However, relying on physical insights, it becomes evident that certain terms can be omitted. Consequently, this simplification enables the development of what are known as reduced

theories, exemplified as follows:

$$\begin{gathered} u_\alpha(\alpha,\beta,z) = u_{\alpha1}(\alpha,\beta) + z^2 u_{\alpha2}(\alpha,\beta) \\ u_\beta(\alpha,\beta,z) = u_{\beta1}(\alpha,\beta) + z u_{\beta2}(\alpha,\beta) + z^2 u_{\beta3}(\alpha,\beta) + z^3 u_{\beta4}(\alpha,\beta) \\ u_z(\alpha,\beta,z) = u_{z1}(\alpha,\beta) + z^4 u_{z2}(\alpha,\beta) \end{gathered} \tag{6}$$

In the CUF literature, the exclusion of a term is achieved through a penalization technique, initiated from a comprehensive uniform theory. As a result, the effective number of terms remains constant. For a more thorough explanation, please consult [16].

2.3 Lagrange-based theories

The section of the shell is approximated with a pattern of Lagrange Points (LPs), which are subdivided into opportune Lagrange polynomials. In this scenario, a LW approach can be employed. Consequently, the 3D displacement field emerges as an interpolation of the displacements calculated at the LPs. The degree of the interpolation is defined by the number of the employed LPs. The number of DOFs equals the sum of the displacements for each LP. The cubic interpolation is used in the paper. Thus, the displacement model can be written as:

$$\begin{gathered} u_\alpha^k(\alpha,\beta,z) = F_{u_x1}^k(z) u_{\alpha1}(\alpha,\beta) + F_{u_x2}^k(z) u_{\alpha2}(\alpha,\beta) + F_{u_x2}^k(z) u_{\alpha3}(\alpha,\beta) + F_{u_x4}^k(z) u_{\alpha4}(\alpha,\beta) \\ u_\beta^k(\alpha,\beta,z) = F_{u_y1}^k(z) u_{\beta1}(\alpha,\beta) + F_{u_y2}^k(z) u_{\beta2}(\alpha,\beta) + F_{u_y3}^k(z) u_{\beta3}(\alpha,\beta) + F_{u_y4}^k(z) u_{\beta4}(\alpha,\beta) \\ u_z^k(\alpha,\beta,z) = F_{u_z1}^k(z) u_{z1}(\alpha,\beta) + F_{u_z2}^k(z) u_{z2}(\alpha,\beta) + F_{u_z3}^k(z) u_{z3}(\alpha,\beta) + F_{u_z4}^k(z) u_{z4}(\alpha,\beta) \end{gathered} \tag{7}$$

See [9] for the mathematical expressions of the interpolation functions.

2.4 Variable kinematic theories

It would be advantageous to utilize a mixed ESL/LW approach to approximate the 3D displacement field. In this approach, certain components employ both Lagrange and Taylor expansions. For instance, the following model could be proposed:

$$\begin{gathered} u_\alpha^k(\alpha,\beta,z) = F_{u_x1}^k u_{\alpha1}(\alpha,\beta) + F_{u_x2}^k u_{\alpha2}(\alpha,\beta) + F_{u_x2}^k u_{\alpha3}(\alpha,\beta) + F_{u_x4}^k u_{\alpha4}(\alpha,\beta) \\ u_\beta(\alpha,\beta,z) = u_{\beta1}(\alpha,\beta) + z u_{\beta2}(\alpha,\beta) + z^2 u_{\beta3}(\alpha,\beta) + z^3 u_{\beta4}(\alpha,\beta) \\ u_z(\alpha,\beta,z) = u_{z1}(\alpha,\beta) + z^4 u_{z2}(\alpha,\beta) \end{gathered} \tag{8}$$

It is important to note that the actual number of terms for the in-plane displacement, u_α^k, relies on the number of layers. Conversely, the 'ESL' terms remain fixed at six.

3 UNIFIED FORMULATION FOR SHELL AND GENERALIZATION TO THE HIGHER-ORDER THEORIES

In the preceding sections, diverse models from the existing literature have been introduced, and there is also the potential to develop new ad hoc models. The CUF demonstrates a distinct capability to concisely characterize these models, from a shared mathematical framework.

In the current formulation, the components of the 3D displacement field are approximated by arbitrary functions defined along the section:

$$\begin{gathered} u_\alpha^k(\alpha,\beta,z) = F_{u_\alpha\tau}^k(z) u_{\alpha_\tau}^k(\alpha,\beta), \text{ with } \tau = 1,\dots, M_{u_\alpha} \\ u_\beta^k(\alpha,\beta,z) = F_{u_\beta\tau}^k(z) u_{\beta_\tau}^k(\alpha,\beta), \text{with } \tau = 1,\dots, M_{u_\beta} \\ u_z^k(\alpha,\beta,z) = F_{u_z\tau}^k(z) u_{z_\tau}^k(\alpha,\beta), \text{with } \tau = 1,\dots, M_{u_z} \end{gathered} \tag{9}$$

$F^k_{u_\alpha\tau}$, $F^k_{u_\beta\tau}$, and $F^k_{u_z\tau}$ represent the expansion functions for the generalized displacements u^k_α, u^k_β, and u^k_z, respectively. In this study, each displacement variable can be discretized by different functions, whereas in previous CUF-based works [9,13,15] the expansions were the for all three components. The symbol τ denotes summation, while M_{u_α}, M_{u_β}, and M_{u_z} are the number of expansions for each displacement variable. The value of τ varies depending on the specific displacement component.

The CUF approximation and the Finite Element Method (FEM) can be successfully integrated to yield numerical results. FEM is utilized to discretize displacements across the mid-surface. Thence, the displacements are written as in the followings:

$$\begin{aligned} u^k_\alpha(\alpha,\beta,z) &= N_i(\alpha,\beta)F^k_{u_\alpha\tau}(z)q^k_{\alpha_{\tau i}}, \text{ with } \tau = 1,\dots, M_{u_\alpha} \text{ and } i = 1,\dots, N_n \\ u^k_\beta(\alpha,\beta,z) &= N_i(\alpha,\beta)F^k_{u_\beta\tau}(z)q^k_{\beta_{\tau i}}, \text{with } \tau = 1,\dots, M_{u_\beta} \text{ and } i = 1,\dots, N_n \\ u^k_z(\alpha,\beta,z) &= N_i(\alpha,\beta)F^k_{u_z\tau}(z)q^k_{z_{\tau i}}, \text{with } \tau = 1,\dots, M_{u_z} \text{ and } i = 1,\dots, N_n \end{aligned} \tag{10}$$

Here, N_i represent the shape functions, with the repeated subscript i signifying summation. N_n denotes the number of shape functions per element. In the present work, the classical nine-node Lagrange (denoted as Q9) element is utilized for numerical assessments. For further details, refer to Bathe [17].

It is also possible to write the three virtual displacements by substituting τ with s and i with j, respectively.

Hereinafter, it is convenient to introduce a succinct notation for both the real and virtual systems, as written below:

$$\begin{aligned} u^k_l(\alpha,\beta,z) &= N_i(\alpha,\beta)F^k_{u_l\tau}(z)q^k_{l_{\tau i}} \\ \delta u^k_m(\alpha,\beta,z) &= N_j(\alpha,\beta)F^k_{u_m s}(z)\delta q^k_{m_{sj}} \end{aligned} \tag{11}$$

Here, l and m can assume the values of α, β, and z. There is no summation over l (or m). This formulation is advantageous for the assembly of the matrices, as illustrated in the subsequent Section 4.

4 GOVERNING EQUATIONS AND FINITE ELEMENT MATRICES

The first step in establishing the governing equations and the FE matrices is to provide the expressions for stress, $\boldsymbol{\sigma}$, and strain, $\boldsymbol{\epsilon}$, tensors. Their vectorial form can be expressed as follows:

$$\boldsymbol{\sigma}^k = \left\{\sigma^k_\alpha, \sigma^k_{\beta\beta}, \sigma^k_{zz}, \sigma^k_{\alpha z}, \sigma^k_{\beta z}, \sigma^k_{\alpha\beta}\right\}^T, \quad \boldsymbol{\epsilon}^k = \left\{\epsilon^k_{\alpha\alpha}, \epsilon^k_{\beta\beta}, \epsilon^k_{zz}, \epsilon^k_{\alpha z}, \epsilon^k_{\beta z}, \epsilon^k_{\alpha\beta}\right\}^T \tag{12}$$

The geometrical relation of strains-displacements reads as:

$$\boldsymbol{\epsilon}^k = \mathbf{D}\mathbf{u}^k \tag{13}$$

where **D** is the matrix of differential operators, see [9] for more information. The constitutive relation for linear elastic orthotropic materials reads as:

$$\boldsymbol{\sigma}^k = \mathbf{C}^k\boldsymbol{\epsilon}^k \tag{14}$$

$\mathbf{C}^k$ is the material elastic matrix, see Bathe [17] for the explicit form.

4.1 Governing equations

The principle of virtual displacement is used to derive the governing equations, which reads:

$$\delta L_{int} = \delta L_{ext} \tag{15}$$

First, the virtual internal work is considered, and its expression is given by:

$$\delta L_{int} = \int_V \delta \boldsymbol{\epsilon}^T \boldsymbol{\sigma}\, dV = \int_V (\delta\epsilon_{\alpha\alpha}\sigma_{\alpha\alpha} + \delta\epsilon_{\beta\beta}\sigma_{\beta\beta} + \delta\epsilon_{zz}\sigma_{zz} + \delta\epsilon_{\beta z}\sigma_{\beta z} + \delta\epsilon_{\alpha z}\sigma_{\alpha z} + \delta\epsilon_{\alpha\beta}\sigma_{\alpha\beta})\, dV \tag{16}$$

where $dV = H_\alpha H_\beta d\alpha d\beta dz$ and $H_\alpha = 1 + z^k/R_\alpha$ and $H_\beta = 1 + z^k/R_\beta$.

Second, considering the virtual external work from point loads:

$$\delta L_{ext} = \delta \mathbf{u}^T \mathbf{P} = \left(\delta u_\alpha P_{u_\alpha} + \delta u_\beta P_{u_\beta} + \delta u_z P_{u_z}\right) \tag{17}$$

After some mathematical manipulations, inserting the CUF and FEM approximations, and the constitutive relations, one can arrive to three distinct governing equations:

$$\begin{aligned}
\delta u^k_{\alpha_{sj}}&: K^k_{u_\alpha u_\alpha s\tau ji} q^k_{\alpha_{\tau i}} + K^k_{u_\alpha u_\beta s\tau ji} q^k_{\beta_{\tau i}} + K^k_{u_\alpha u_z s\tau ji} q^k_{z_{\tau i}} = P^k_{u_\alpha sj} \\
\delta u^k_{\beta_{sj}}&: K^k_{u_\beta u_\alpha s\tau ji} q^k_{\alpha_{\tau i}} + K^k_{u_\beta u_\beta s\tau ji} q^k_{\beta_{\tau i}} + K^k_{u_\beta u_z s\tau ji} q^k_{z_{\tau i}} = P^k_{u_\beta sj} \\
\delta u^k_{z_{sj}}&: K^k_{u_z u_\alpha s\tau ji} q^k_{\alpha_{\tau i}} + K^k_{u_z u_\beta s\tau ji} q^k_{\beta_{\tau i}} + K^k_{u_z u_z s\tau ji} q^k_{z_{\tau i}} = P^k_{u_z sj}
\end{aligned} \tag{18}$$

In this work, the Mixed Interpolation of Tensorial Component (MITC) method is employed to address shear locking issues. For brevity, the extended formulation is not provided here. Please refer to [13] for more information.

The core of the stiffness matrix is represented by the scalar $K_{u_m u_l s\tau ji}$. In CUF terminology, it is termed the Fundamental Nucleus (FN). Thence, the stiffness matrix can be composed of nine independent scalar parameters. This variable-kinematics approach has been proposed in a companion paper concerning shell formulation for isotropic structures [18]. In contrast, previous CUF-based papers [15] used a submatrix $\mathbf{K}_{s\tau ji}$ with dimensions 3×3 as the kernel, where the same expansion theory was used for all the three displacement components. In this latter method, the scalar $K_{u_m u_l}$ is a component of the matrix $\mathbf{K}_{s\tau ji}$.

4.2 Assembly of the Stiffness Matrix and Load Vector

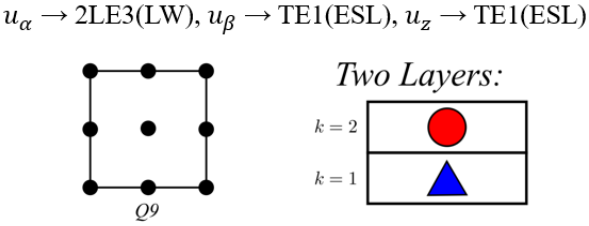

Figure 2: Example of a shell element. u_α is studied by using two quadratic Lagrange elements, whereas a linear model (TE1) approximates the displacement variables u_β and u_z.

This subsection delineates the process of assembling the stiffness matrix and the load vector through an example. Figure 2 shows a nine-node element (Q9) is depicted and the structural theories employed. In particular, u_α is approximated by two quadratic Lagrange sectional elements (2LE3, LW), while the ESL TE1 model is used for u_β and u_z. Consequently, $M_{u_\alpha} =$

5, $M_{u_\beta} = 2$, and $M_{u_z} = 2$. Note that the number of expansions for u_α is five because there are five LPs along the thickness. Thus, nine degrees of freedom are assigned to each FE node, resulting in a total of 81 degrees of freedom. In Fig. 3, the stiffness matrix, with dimensions 81×81, and the load vector, with dimensions 81, for the entire structure are illustrated.

Each submatrix $\mathbf{K}_{ji}$ is further divided into nine submatrices, while each subvector $\mathbf{P}_j$ is composed of three smaller subarrays. For instance, Fig. 4 illustrates clearly the nine components of $\mathbf{K}_{11}$ and the three components of $\mathbf{P}_1$. It is important to note that the dimension and shape of the matrices $\mathbf{K}_{u_m u_l 11}$ depend on the number of terms in the models adopted for each displacement variable. The use of different number of terms for the variables may lead to rectangular sub-matrices $\mathbf{K}_{u_m u_l 11}$ with varying dimensions. It is worth noting that these submatrices may be LW (e.g. $\mathbf{K}_{u_\alpha u_\alpha 11}$), ESL (e.g. $\mathbf{K}_{u_\beta u_\beta 11}$), or mixed ESL/LW (e.g. $\mathbf{K}_{u_\alpha u_\beta 11}$). Finally, each 1×1 scalar FN corresponds to the core of the matrices. A similar procedure can be followed for the load array.

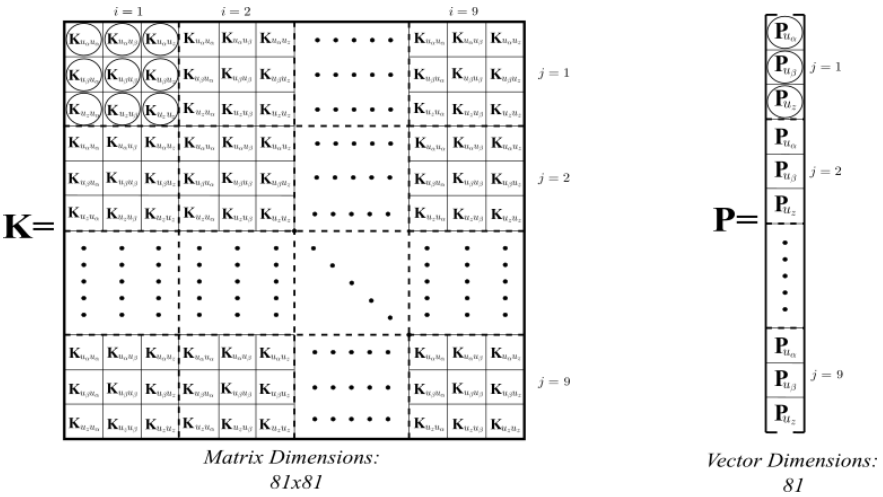

Figure 3: Assembly of the general stiffness matrix and the general load vector.

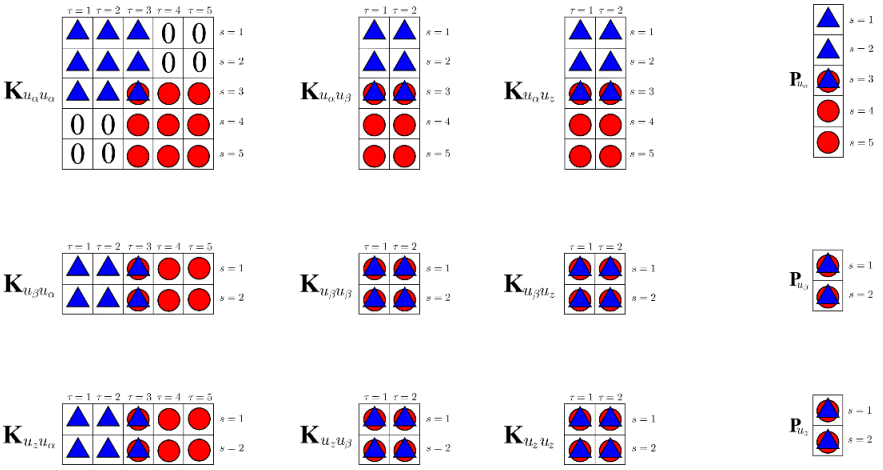

Figure 4: Assembly of the stiffness matrix (submatrix $\mathbf{K}_{11}$) and the load vector (subvector $\mathbf{P}_1$).

5 NUMERICAL RESULTS

This section explores two benchmarks that focus on the study of displacements and stresses. Additionally, both thick and thin structures are considered. Since the present method can build many theories, a consistent acronym system is proposed.

As seen previously, several types of models and polynomials are considered. When the uniform Taylor expansion is used, the following notation is adopted: TEn where n indicates the polynomial order. For the Lagrange expansion, the label LEp is used, where p is the number of LPs for each Lagrange elements. When the reduced models are utilized, they are explicitly defined during the expositions of the benchmarks in the tables. It is also possible to completely disregard the terms for one displacement component, and this is indicated by a '0'.

5.1 Bending of a two-layered shell

The first benchmark considered is a cylindrical two-layered shell ([90°/0°] is the stacking sequence), with geometrical properties outlined in Fig. 5. The ratio $R_\beta/b = \pi/3$ and a is unity. Shells of radius-to-thickness ratios $R_\beta/h = 4$ (thick) and $R_\beta/h = 100$ (thin) are considered. The analytical reference solution, denoted as 'Exact', is obtained from Ren [19]. The material is orthotropic with the following properties: $E_L/E_T = 25$, $E_T/E_3 = 1$, $\nu_{LT} = \nu_{T3} = \nu_{L3} = 0.25$, $G_{LT}/E_T = G_{L3}/E_T = 0.5$, $G_{T3}/E_T = 0.2$, where 'L', 'T' and '3' indicate the longitudinal, transverse, and the out-of-plane direction, respectively. The shell, simply supported on the edges along the α axis, is subjected to a sinusoidal pressure $p = P_z \sin(\pi\beta/b)$ with a mechanical load amplitude of $P_z = 1$ [Pa] at the top position.

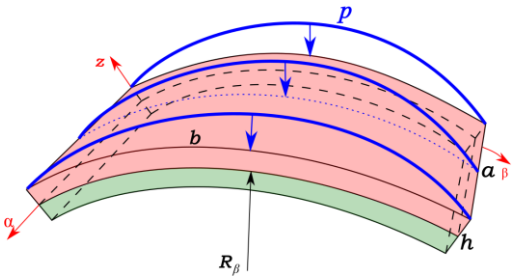

Figure 5: Geometrical properties and loading conditions of a two-layered shell taken from Ren [19]

The study assesses transverse displacements, u_z, along with in-plane stress, $\sigma_{\beta\beta}$, shear stress, $\sigma_{\beta z}$, and transverse normal stresses, σ_{zz}. Specifically, u_z, $\sigma_{\beta\beta}$, and σ_{zz} are calculated in [a/2, b/2, z], while $\sigma_{\beta z}$ is evaluated in [0, b/2, z]. The results are presented in a non-dimensional form for comparison purposes, as follows:

$$\bar{u}_z = \frac{10E_T u_z}{P_z h\left(\frac{R_\beta}{h}\right)^4} \qquad \bar{\sigma}_{\beta\beta} = \frac{\sigma_{\beta\beta}}{P_z\left(\frac{R_\beta}{h}\right)^2} \qquad \bar{\sigma}_{\beta z} = \frac{\sigma_{\beta z}}{P_z\left(\frac{R_\beta}{h}\right)} \qquad \bar{\sigma}_{zz} = \frac{\sigma_{zz}}{P_z} \tag{19}$$

The convergence analysis is omitted here for brevity. Mesh 1×15 MITCQ9 is utilized for the thick case, whereas Mesh 1×20 MITCQ9 is employed for the thin shell. Regarding the section discretization, two Lagrange elements are adopted for each material layer.

Tables 1 and 2 present the results for the thick and thin shell, respectively. The first three

columns indicate the expansions used for the displacement variables. Subsequently, the results for the displacements and stresses are depicted. The Degrees of Freedom (DOFs) are also provided. Finally, under the Notes label, the nomenclature of 'ad hoc' theories is provided for clarity. The first rows present the uniform models, followed by the ESL/LW models.

Table 1: Two-layered shell. Case $R_\beta/h = 4$. Transverse displacements evaluated in [a/2, b/2, 0], in-plane stresses evaluated in [a/2, b/2, h/2], and shear stresses evaluated in [a/2, 0, 0].

Expansions			Results				
u_α	u_β	u_z	$\bar{u}_z$	$\bar{\sigma}_{\beta\beta}$	$\bar{\sigma}_{\beta z}$	DOF	Notes
			Exact [19]				
—	—	—	0.854	2.511	0.871	—	
			Uniform Models				
LE4	LE4	LE4	0.854	2.506	0.868	3627	
TE1	TE1	TE1	0.804	2.276	0.585	558	
TE2	TE2	TE2	0.782	2.163	0.631	837	
			ESL/LW Models				
0	LE4	LE4	0.854	2.506	0.868	2418	Model 1
TE1	LE4	TE1	0.835	2.479	0.866	1581	
0	LE4	TE1	0.835	2.479	0.866	1395	Model 2
TE2	LE4	TE2	0.848	2.506	0.869	1797	
0	LE4	$u_{z1} + z^2 u_{z2}$	0.850	2.454	0.866	1395	Model 3

Table 2: Two-layered shell. Case $R_\beta/h = 100$. Transverse displacements evaluated in [a/2, b/2, 0], in-plane stresses evaluated in [a/2, b/2, h/2], and shear stresses evaluated in [a/2, 0, 0].

Expansions			Results				
u_α	u_β	u_z	$\bar{u}_z$	$\bar{\sigma}_{\beta\beta}$	$\bar{\sigma}_{\beta z}$	DOF	Notes
			Exact [19]				
—	—	—	0.403	2.165	0.867	—	
			Uniform Models				
LE4	LE4	LE4	0.403	2.162	0.869	4797	
TE1	TE1	TE1	0.396	2.141	0.542	738	
TE2	TE2	TE2	0.403	2.162	0.579	1107	
			ESL/LW Models				
0	LE4	LE4	0.403	2.162	0.869	3534	Model 1
TE1	LE4	TE1	0.396	2.142	0.862	2091	
0	LE4	TE1	0.396	2.142	0.862	1845	Model 2
TE2	LE4	TE2	0.403	2.163	0.869	2337	
0	LE4	$u_{z1} + z^2 u_{z2}$	0.400	2.148	0.865	1845	Model 3

Figures 3 and 4 show the trends of the stresses for thick and thin shells, respectively. In particular, Figs. 3 (a) and 4 (a) study the in-plane stresses, $\sigma_{\beta\beta}$. Figs. 3 (b) and 4 (b) illustrate the shear stresses, $\sigma_{\beta z}$, while Figs. 3 (c) and 4 (c) show the transverse normal stresses, σ_{zz}. The results clearly shows that the LW approach for the displacement u_β is needed. It is demonstrated that the in-plane displacement u_α does not influence the output. The LW approach for the

displacement u_z is mandatory if the transverse stresses are required, while for the determination of the other outcomes, few terms are sufficient. It is also shown how the ratio R_β/h influences the results, especially the transverse displacement and the out-of-plane stresses $\sigma_{\beta z}$.

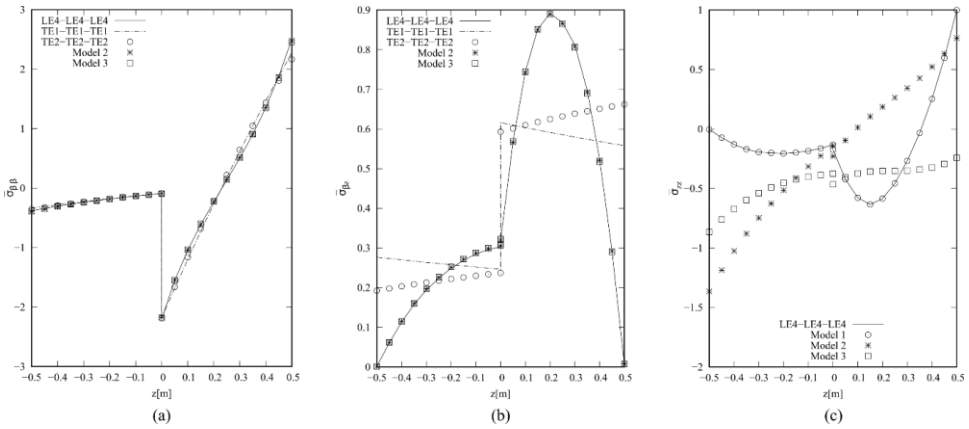

Figure 6: Two-layered shell. Case $R_\beta/h = 4$. In-plane stresses (a) evaluated in [a/2, b/2, z]. Shear stresses (b) evaluated in [a/2, 0, z]. Normal stresses (c) evaluated in [a/2, b/2, z].

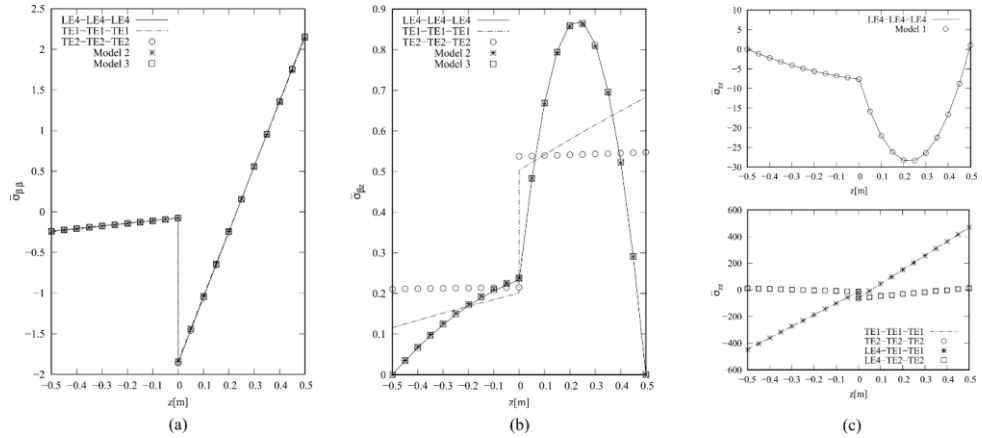

Figure 7: Two-layered shell. Case $R_\beta/h = 100$. In-plane stresses (a) evaluated in [a/2, b/2, z]. Shear stresses (b) evaluated in [a/2, 0, z]. Normal stresses (c) evaluated in [a/2, b/2, z].

5.2 Bending of a three-layered shell

A three-layered cylindrical shell is studied as the second benchmark. The geometrical properties and the material are the same of the previous example. Also, the boundary and loading conditions have been presented before. Now, the stacking sequence is: [90°/0°/90°]. For the sake of brevity, only the thick $R_\beta/h = 4$ shell was considered.

Mesh 1×15 MITCQ9 is used for the thick case. Considering the section discretization, two Lagrange element are adopted for each material layer.

Table 3 illustrates the results for the thick shell. It mirrors the structures of the Tables in the preceding subsection. Figure 8 (a) studies the in-plane stresses, $\sigma_{\beta\beta}$. Figure 8 (b) illustrates the shear stresses, $\sigma_{\beta z}$, while Fig. 8 (c) shows the transverse normal stresses, σ_{zz}. Also, this example

shows that each displacement component may be approximated in different way. Here, also the stresses $\sigma_{\beta\beta}$ are greatly influenced by the choice of the polynomials and approaches.

Table 3: Three-layered shell. Case $R_\beta/h = 4$. Transverse displacements evaluated in [a/2, b/2, 0], in-plane stresses evaluated in [a/2, b/2, h/2], and shear stresses evaluated in [a/2, 0, 0].

Expansions			Results				
u_α	u_β	u_z	$\bar{u}_z$	$\bar{\sigma}_{\beta\beta}$	$\bar{\sigma}_{\beta z}$	DOF	Notes
			Exact [19]				
—	—	—	0.457	1.367	0.476	—	
			Uniform Models				
LE4	LE4	LE4	0.458	1.364	0.477	5301	
TE1	TE1	TE1	0.331	0.797	0.209	558	
TE2	TE2	TE2	0.329	0.768	0.210	837	
			ESL/LW Models				
0	LE4	LE4	0.458	1.364	0.477	3534	Model 1
TE1	LE4	TE1	0.459	1.334	0.477	2139	
0	LE4	TE1	0.459	1.334	0.477	1953	Model 2
TE2	LE4	TE2	0.458	1.357	0.477	2325	
0	LE4	$u_{z1} + z^2 u_{z2}$	0.458	1.356	0.477	1953	Model 3

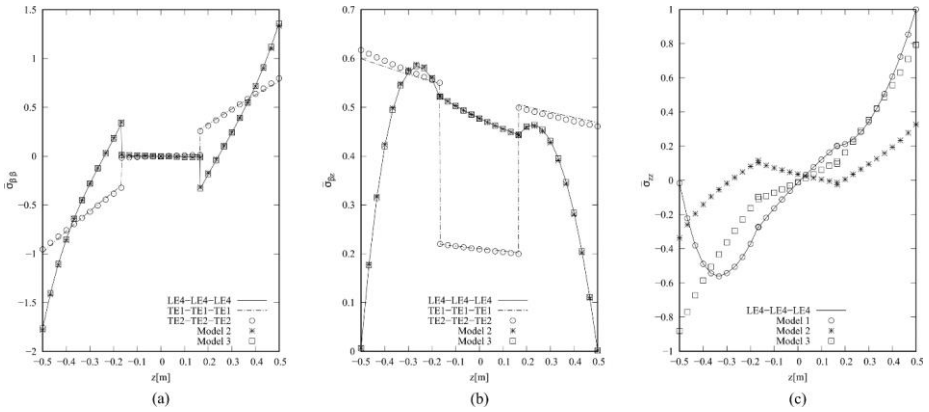

Figure 8: Three-layered shell. Case $R_\beta/h = 4$. In-plane stresses (a) evaluated in [a/2, b/2, z]. Shear stresses (b) evaluated in [a/2, 0, z]. Normal stresses (c) evaluated in [a/2, b/2, z].

6 CONCLUSIONS

This paper introduces a novel approach to constructing theories for multi-layered shells within the framework of the CUF. This innovative approach enables the development of specialized structural theories for each displacement variable, facilitating the creation of tailored 2D Finite Element models. Two benchmarks are investigated to evaluate the method, with analytical literature solutions serving as references. The analysis encompasses structures with varying thicknesses and loading conditions, focusing on simply supported shells. Based on the results obtained throughout the paper, the following conclusions can be drawn:

- It is possible to reduce computational costs using only the significant terms in the structural theories;

- The number of effective variables depends largely on the specific problem;
- Mixed ESL/LW approach is an incredible accelerator;
- Both thick and thin structures can be efficiently analyzed.

REFERENCES

[1] Carrera, E. Historical review of zig-zag theories for multilayered plates and shells. *Appl. Mech. Rev.* (2003) **56**(3):287-308.

[2] Reissner, E. The effect of transverse shear deformation on the bending of elastic plates. *J. Appl. Mech.* (1945) **12**:69-77.

[3] Mindlin, R. Influence of rotary inertia and shear flexural motion of isotropic, elastic plates. *J. Appl. Mech.* (1951) **18**:31-38.

[4] Kirchhoff, G. Über das gleichgewicht und die bewegung einer elastischen scheibe. *J. Reine Angew. Math.* (1850) **40**:51-88.

[5] Kant, T. and Owen, D.R.J. and Zienkiewicz, O.C. A refined higher-order C° plate bending element. *Comput. Struct.* (1982) **15**(2):177-183.

[6] Reddy, J.N. *Mechanics of Laminated Composite Plates and Shells: Theory and Analysis*. CRC Press, (1997).

[7] Reddy, J.N. An evaluation of equivalent-single-layer and layerwise theories of composite laminates. *Compos. Struct.* (1993) **25**:21-35.

[8] Noor, A.K. and Burton, W.S. Assessment of computational models for multilayered composite shells. *Appl. Mech. Rev.* (1990) **43**:67-97.

[9] Carrera, E. and Cinefra, M. and Petrolo, M. and Zappino, E. *Finite element analysis of structures through unified formulation*. John Wiley & Sons, (2014).

[10] Carrera, E. Multilayered shell theories accounting for layerwise mixed description, Part 1: Governing equations. *AIAA J.* (1999) **37**(9):1107–1116.

[11] Carrera, E. Multilayered shell theories accounting for layerwise mixed description, Part 2: Numerical evaluations. *AIAA J.* (1999) **37**(9):1117–1124.

[12] Bucalem, M.L. and Bathe, K.J. Higher-order MITC general shell elements. *Int. J. Num. Meth. Engng*. (1993) **36**(21):3729-3754.

[13] Cinefra, M. and Carrera, E. Shell finite elements with different through-the-thickness kinematics for the linear analysis of cylindrical multilayered structures. *Int. J. Num. Meth. Engng*. (2013) **93**(2):160-182.

[14] Lo, K.H. and Christensen, R.M. and Wu, E.M. A High-Order Theory of Plate Deformation Part 1: Homogeneous Plates. *J. Appl. Mech.* (1977) **44**(4):663-668.

[15] Carrera, E. Developments, ideas, and evaluations based upon Reissner's Mixed Variational Theorem in the modeling of multilayered plates and shells. *Appl. Mech. Rev.* (2001) **54**(4):301-329.

[16] M. Petrolo and E. Carrera. Best theory diagrams for multilayered structures via shell finite elements. *Adv. Model. Simul. Eng. Sci*. (2019) **6**(4):1-23.

[17] Bathe, K.J. *Finite Element Procedure.* Prentice Hall, (1996).

[18] Carrera, E. and Scano, D. and Zappino, E. Shell Finite Elements with Variable Structural Approximations. *To be Submitted*.

[19] Ren, J.G. Exact solutions for laminated cylindrical shells in cylindrical bending. *Compos. Sci. Technol.* (1987) **29**(3):169-187.